IJMA

International Journal of Medical Arts

VOLUME 6, ISSUE 8, AUGUST 2024

P- ISSN: 2636-4174
E- ISSN: 2682-3780

Available online at Journal Website
https://ijma.journals.ekb.eg/
Main Subject [Basic Sciences]

Original Article

Covering and the Manufacture of *Myxopyronin B* Antibiotic from Assorted Soil Environments in Egypt

Mohammed M. Kassab *

Department of Microbiology and Immunology, Faculty of Pharmacy, Cairo University, Giza, Egypt

Article information

Received: 09-02-2024

Accepted: 11-06-2024

DOI: 10.21608/ijma.2024.268945.1932.

*Corresponding author

Email: ksabmhmd676@gmail.com

Citation: Kassab MM. Covering and the Manufacture of Myxopyronin B Antibiotic from Assorted Soil Environments in Egypt. IJMA 2024; August; 6 [8]:4834-4847 , doi: 10.21608/ijma.2024.268945.1932.

ABSTRACT

BACKGROUND: Across the world, antibiotic resistance is a grave problem.

AIM OF THE STUDY: To explore Egypt's diverse soil habitats for the production of bacterial *Myxopyronin B*, which is then tested for antimicrobial activity in *preclinical animal studies* and *randomized human clinical trials stages 1/2*.

METHODOLOGY: Egypt's various soil conditions were examined for the development of bacterial isolates that produced the antibiotic compound *Myxopyronin B.* To determine the test antibiotic's *minimum inhibitory concentration* [*MIC*] and in vitro antibacterial activity, *the Broth microdilution method* and *the Paper disc diffusion assay* were utilized. Moreover, in vivo *antibacterial spectrum*, *adverse medication responses*, and *pharmacokinetics* were found in *preclinical animal testing stages*; as well as *phases 1/2* of *randomized clinical studies* involving 150 volunteer humans from both secs with ages ranging from 5-60 years old.

RESULTS: *Myxopyronin B* was generated from the culture supernatant of *Myxococcus SDU36*, the main soil bacterial isolate cultured on *a Casein yeast peptone plate*. With *MICs* less than *100 mcg/ml*, the test antibiotic prevented the growth of several *Gram +ve* bacteria, whereas, at *MICs* higher than *100 mcg/ml*, it inhibited the growth of a small number of *Gram -ve* bacteria, including Escherichia coli. However, eukaryotic cells—such as those found in fungi and humans—were unaffected. The test antibiotic was seen to inhibit prokaryotic *DNA-dependent RNA polymerase [RNLP]*, indicating its *bactericidal activity*. Mean *Cmax* was *9-10 mcg/ ml* at mean *Tmax 1* hour when 6*00 mg* dose was orally administered in *randomized human clinical trials phases 1/2; as well as T1/2* reached *2.25 hours* following *first-order kinetics of elimination*. The duration of its action was nearly *8 hours* after oral administration.

CONCLUSION: The present study was promising due to the production of the bactericidal antibiotic *Myxopyronin B* from *Myxococcus sp. SDU36* isolated from different soil environments in Egypt.

Keywords: *Myxopyronin B*; Microbial; Antibiotic; Resistance; Myxobacteria.

INTRODUCTION

For an antibiotic to be useful as a medicine, it must exhibit selective toxicity [1]. The activities of bacteria must be significantly suppressed compared to those of human cells [2]. The search for novel antibiotic sources is essential because antibiotic resistance is a serious, global issue that has to be addressed [3].

Cell walls, ribosomes, cell membranes, and nucleic acids are the four main targets of antibacterial drugs [4]. These drugs have no impact on human cells since they don't have a cell wall and have unique ribosomes, nucleic acid enzymes, and sterols in their membranes [5]. Drugs known to be *bactericidal* are effective against bacteria [6]. Conversely, bacteriostatic drugs prevent the growth of germs [7]. The pathogen is eliminated by the patient's phagocytes while using bacteriostatic drugs [8].

When a patient has a low neutrophil count, they should be given bactericidal drugs [9]. The alpha-pyrone antibiotic class includes *Myxopyronins* [10]. The term "*pyrones*" or "*pyranones*" refers to a class of heterocyclic chemical compounds [11]. They comprise an unsaturated six-membered ring that is composed of one oxygen atom and a ketone functional group [12]. The names of the two isomers are *2-pyrone* and *4-pyrone* [13]. Given that *Myxopyronins* exhibit no cross-resistance with other medications, they may be able to mitigate the growing problem of drug resistance in tuberculosis [14]. Additionally, their medication may be beneficial for *Methicillin-resistant Staphylococcus aureus* [*MRSA*] [15].

Assessing the production of a novel antibiotic, *Myxopyronin B*, in various soil conditions in Egypt was the aim of the present investigation. It was also examined for antibacterial efficacy in *phases 1/2 randomized human clinical trials*.

PATIENTS AND METHODS

Ethical statement: Prioritized in the current study were all pertinent institutional, national, and/or international standards concerning the use and care of humans and animals. All study protocols involving humans and animals were authorized by the Ethical Committee for Human and Animal Handling at Cairo University [*ECAHCU*], located at the Faculty of Pharmacy, Cairo University, Egypt, by the Weather all Report's recommendations [approval number *TX10/2023*]. At all costs, the study's human and animal subjects' numbers and suffering were kept to a minimum. *Phases 1/2* registration number for the randomized human clinical trials was *NCT00000806/ 2023*.

Type of the study: Screening experimental study.

Place and date of the study: This study was processed at the faculty of pharmacy, Cairo University, Egypt between *May 2023* and February *2024*.

Source of animal models: They were existed and legalized by the pharmacology and toxicology department of the faculty of pharmacy, at Cairo University, Egypt.

Inclusion criteria for animal models: A hundred adult male obese rabbit animal models weighing about *2 kg*; could be inoculated with different bacterial infections. Rabbits were acclimatized for one week before the experiment. At a humidity [*50 % ± 5*], light-dark cycle [*12/ 12 h*], and a controlled temperature [$25 \pm 2\ ^{\circ}C$]. The rabbits were fed with fresh grass.

Exclusion criteria for animal models: Young and female rabbits; Non-obese rabbits weighing less than *2 kg*.

Collection of 100 soil samples: Randomly selected samples were grassland soils collected from various soil types in Egypt at a depth of *30 cm*. Before processing, samples were stored at $4^{o}C$ in sterile containers. Each soil sample was weighed *one gram* and each *250 ml Erlenmeyer flask* contained *99 ml* of sterile distilled water. The vials were shaken at *400 rpm* using *a gyroscopic shaker* for *5 min*. After dilution from 10^{-1} to 10^{-6} in sterile distilled water, the soil suspension was placed on selective casein peptone [*CYP*] yeast agar medium [purchased from Sigma-Aldrich, USA]. 50 cc of nutrient broth with *pH 7* was added to a *250 ml Erlenmeyer flask* to create an inoculum for the bacterial strain under study. The medium was autoclaved and then inoculated with a loop of culture from nutrient agar slants overnight. The inoculum consisted of inoculated vials, which were shaken throughout the day at *150 rpm*.

Instruments

Table [1]: List of instruments

Instrument	Model and manufacturer
Autoclaves	*Tomy, japan*
Aerobic incubator	*Sanyo, Japan*
Digital balance	*Mettler Toledo, Switzerland*
Oven	*Binder, Germany*
Deep freezer -70℃	*Artiko*
Refrigerator 5	*whirlpool*
PH meter electrode	*Mettler-toledo, UK*
Deep freezer -20℃	*whirlpool*
Gyrator shaker	*Corning gyrator shaker, Japan*
190-1100nm Ultraviolet-visible spectrophotometer	*UV1600PC, China*
Light[optical] microscope	*Amscope 120X-1200X, China*

Materials: All chemical and biochemical substances were obtained from Algomhuria Pharmaceutical Company and Alnasr Chemical Company, Egypt. All chemical reagents utilized were of expository review.

Isolation of *Myxococcus SDU36* producing *Myxopyronin B* antibiotic: The selective isolation of species of *Myxococcus SDU36* from different soil samples was directly performed utilizing *dilution plating*. The technique included the suppression of competing bacteria exploiting antibiotics such as *10 mcg/ ml Vancomycin* and/ or *10 mcg/ ml Chloramphenicol*

combined with wet heat treatment of soils and air drying. Fungi were eliminated by supplementing the plating medium with *2 mcg/ ml Terbinafine HCl*. Swarming of *Myxococcus SDU36* colonies was controlled with *Casein Yeast Peptone* [*CYP*] plates incubated at *30°C* and *PH 7.2* for *5 days*. The composition of *the CYP* plate included *0.4 % Peptone* from *Casein*, tryptically digested, *0.3 % CaCl2. 2H2O, and 0.1% MgSO4.7H2O, PH 7.2*. The potent bacterial isolate producing *Myxopyronin* was performed utilizing *a 16 S rRNA* sequencing technique. The predominant bacterial isolate with high antibacterial activity was identified using *16S rRNA* sequencing and other biochemical tests. Nucleic acid was extracted from a swab by bead-beating in a buffered solution containing Phenol, Chloroform, and Isoamyl alcohol. The variable region of *the 16S rRNA* gene was then amplified from the resulting nucleic acid using *PCR*. The genomic *DNA* was extracted from *120 hours of* cultured cells using a *DNA purification kit* [*PurreLink™ Genomic DNA Mini Kit with Catalog number: K182002* was purchased from Invitrogen, USA] according to the protocol provided by the manufacturer of *the DNA* purification kit. *The 16S rRNA gene* was amplified by *PCR* [*PCR* SuperMix kit was purchased from Invitrogen, *USA*] using forward [*5`-AGAGTTTGATCCTGGCTCAG-3`*] and reverse [*5-GGTTACCTTGTTACGACTT-3`*] *primers*. *PCR* amplicons from up to hundreds of samples were then combined and sequenced on a single run. The resulting sequences were matched to a reference database to determine relative bacterial abundances. Polymerase Chain Reaction [*PCR*] was a powerful method for amplifying particular segments of *DNA*. *PCR* used the enzyme *Platinum™ Taq DNA polymerase* with catalog number *10966018* [purchased from Invitrogen, *USA*] that directed the synthesis of *DNA* from deoxynucleotide substrates on a single-stranded *DNA template*. *DNA polymerase* added nucleotides to the 3` end of a custom-designed oligonucleotide when it was annealed to a longer template *DNA*. Thus, if a synthetic oligonucleotide was annealed to a single-stranded template that contained a region complementary to the oligonucleotide, *DNA polymerase* could use the oligo-nucleotide as a primer and elongate its 3` end to generate an extended region of double-stranded *DNA*. Denaturation was the initial *PCR* cycle stage The *DNA* template was heated to *94° C*. This broke down the weak hydrogen bonds that held *DNA* strands together in a helix, allowing the strands to separate creating single-stranded *DNA*. Annealing was the second *PCR* cycle. The mixture was cooled to anywhere from *50-70° C*. This allowed the primers to bind [anneal] to their complementary sequence in the template *DNA*. The extension was the final step of *the PCR* cycle. The reaction was; then heated up to *72° C*, the optimal temperature for *DNA polymerase* to act. *DNA polymeras*e extended the primers, adding nucleotides onto the primer in a sequential manner, using the target *DNA* as a template. With one cycle, a single segment of double-stranded *DNA* template was amplified into two separate pieces of double-stranded *DNA*. These two pieces were then available for amplification in the next cycle. As the cycles were repeated, more and more copies were generated and the number of copies of the template was increased exponentially. The amplified *PCR* product was sequenced using a genetic analyzer *3130XL* [purchased from Applied Biosystems, *USA*]. *DNA* sequence homology search analysis of the predominant bacterial isolate was achieved using the Blastn algorithm at the *NCBI* website. Fruiting bodies were examined using a *Stereomicroscope* [*dissecting microscope*] *MSC-ST45T* [purchased from Infetik, China]. Wet mounts from crushed fruiting bodies were prepared. The refractivity, shape, and size of *Myxospores* were determined by victimizing phase contrast microscopy. On the other hand, the plates were exposed to *360 nm* wavelength ultraviolet light to assess the fruiting bodies fluoresced [16].

Identification *of Myxopyronin B*-producing bacterial isolates:

Gram stain: It grouped bacteria into two types based on their cell wall composition. Bacterial cells turned purple after being treated with a solution of *crystal violet* and then *iodine* on a microscope slide. When stained cells were treated with solvents such as alcohol or acetone, *Gram-positive* bacteria retained the stain while *Gram-negative* bacteria lost the stain and became colorless. With the addition of the decolorizing agent *safranin*, the transparent Gram-negative bacteria turned pink [17].

Spore shape: This was discovered using the spore staining method. To get rid of any fingerprints, the slide was wiped with alcohol and a Kim wipe. On the bottom of the slide, a Sharpie was used to create two circles. Each circle was filled with two tiny droplets of water using an inoculation loop. A very small amount of germs was taken out of the culture tube using an aseptic method. The water droplet on the slide had microorganisms on it. The slide was thoroughly dried by air. Bypassing the slide through the flame three to four times with the smear side up, the slide was heat-fixed. It took a while for the slide to completely cool. A piece of paper towel placed inside the slide's border was used to hide the streaks. A beaker of heating water was situated over the slide. The slide was allowed to steam for three to five minutes; while the paper towel was covered with a malachite green liquid. Removed and thrown away was the discolored paper towel. To get rid of any stray paper towel bits, the slide was gently cleaned with water. The counter-stain was safranin for 1 minute. Before putting the slide on the microscope's stage and seeing it via the oil immersion lens, the slide's bottom was dried [18].

Spore site: During the Gram stain test, the spore location was grooved [19].

Cell shape: During the Gram stain test, the cell shape was determined [20].

Blood hemolysis: On blood agar media, the test antibiotic capacity to haemolyze the blood was tried [21].

Motility test: It distinguished between motile bacteria and non-motile bacteria. A sterile needle was used to penetrate the medium to within *1 cm* of the tube's bottom to select a well-isolated colony and test for motility. The needle was certainly preserved in the same position as it was artifact-ed and removed from the medium. It took *18* hours of incubation at *35°C*, or until evident growth materialized [22].

Nitrate reduction test: *0.5 ml* of *Nitrate broth* situated in a clean test tube was autoclaved for *15 minutes* at *15 lbs pressure* and *121°C* and was allowed to cool to room temperature. The tube was inoculated with a heavy inoculum of unspoiled bacterial culture and was incubated at *35°C* for *2 hours*. *2 drops* of *reagent A* and *2 drops* of *reagent B* were added and blended well. The evolution of the red color within *2 minutes* was ascertained. If no red color was formed, a small quantity of Z*inc dust* was added and discovered for the alteration to the red color in *5 minutes* [23].

Methyl red test: In the *Methyl Red* test, a pestiferous tube of MR broth was used before adding the methyl red *PH* indicator. The buffers in the medium were over by the acids when an organism utilized the blended acid fermentation pathway and brought forth stable acidic end products, consequent on an acidic environment [24].

Catalase test: A little inoculum of a specific bacterial strain was enclosed in a *3% Hydrogen peroxide* solution to comprehend if it might produce *Catalase*. It was ascertained that the rapid emission of *Oxygen bubbles* [25].

Oxidase test: The *1% Kovács oxidase reagent* was added to a little piece of filter paper, which was then let to air dry. A well-isolated colony was confiscated from a fresh [*18 to 24-hour culture*] bacterial plate victimizing a sterile loop, and it was then hung up onto processed filter paper. Color changes were detected [26].

Citrate utilization: Five milliliters of a *Simmon Koser's citrate* medium were condemned after it had been autoclaved at *15* pounds for *15 minutes*. To make up a clear slant and butt, the test tube incorporating melted citrate medium was slanted. Exploiting sterilized wire and labeled tubes, the specified samples of microbe were injected on the media's incline. For *24 hours*, the tubes were incubated at *37°C*. The medium's color alteration was observed [27].

Starch hydrolysis: For *48 hours* at *37°C*, the bacterium plates were injected. After incubation, a dropper was utilized to saturate the surface of the plates with an iodine solution for *30 seconds*. Iodine that was superfluous was subsequently swarmed out. The area surrounding the bacterial growth line was dictated [28].

Tween 80 hydrolysis: *1% Tween 80* was exploited to make up agar media. The rendered microorganism was introduced to the *Tween 80 agar plates* by employing an inoculating loop to make up a single center streak in the plate. The plates were procreated for *24* hours at *37 °C*. *HgCl2* solution was displaced over the plates. After a short while, the plates were discovered. Positive test outcome; A well-defined halo-zone surrounding the injected area demonstrated a *Tween 80* chemical reaction [29].

Growth at 10-45 ^{0}C: On nutrient agar media, the biological process was observed to be possible at 10- *45°C* [30].

Indole test: The test tube incorporating the microorganism for inoculation received *5 drops* of the *Kovács reagent* directly. Within seconds after inserting the reagent into the media, the reagent layer settled a pink to red color [cherry-red ring], which was a mark of a positive *Indol test* [31].

Tolerance salinity test: Its capacity to evolve on nutrient agar while being responsive to *5% &7% NaCl* was detected [32].

Voges-Proskauer [VP] test: For the test, *Voges-Proskauer broth*, a glucose-phosphate broth affluent-ed with microorganisms, was added to *Alpha-naphtho*l and *Potassium hydroxide*. A successful consequence was betokened aside a *Cherry red tint;* whereas an unfortunate consequence was signal via a yellow-brown color [33].

Casein hydrolysis test: For testing the *Casein* hydrolyzing activity of the test antibiotic, a single line streak of the given culture was performed in the center of the skim milk agar plate under aseptic conditions and the plate was procreated at *37°C* in an incubator for *24-48 h* [34].

Saccharide fermentation tests:

Glucose fermentation test: The fermentation reactions of glucose were investigated using glucose purple broth. Peptone and the *PH* indicator bromcresol purple made up the purple broth. A *1%* concentration of glucose was added. Isolated colonies from a 24-hour pure culture of microorganisms were added to the glucose purple broth as an inoculant. Parallel to the inoculation of the glucose-based medium, a control tube of purple broth base was used. The inoculated medium was incubated aerobically for *3 days* at *35–37* °C. The medium began to become yellow, which was a sign of a successful outcome. A poor carbohydrate fermentation response was indicated by the lack of yellow color development [35].

Fructose fermentation test: A pure culture's inoculum was aseptically transferred to a sterile tube of phenol red fructose broth. The infected tube was incubated for *18–24 hours* at *35–37 °C*. A color shift from red to yellow, signifying acidic pH alteration, was a sign of a favorable response [36].

Maltose fermentation test: A pure culture inoculum was aseptically transferred to a sterile tube containing phenol red maltose broth. The infected tube was incubated for *18–24 hours* at *35–37 °C*. A color shift from red to yellow, signifying an acidic PH alteration, was a sign of a favorable response [37].

Sucrose fermentation test: A pure culture's inoculum was aseptically transferred to a sterile tube containing phenol red sucrose broth. For *24 hours*, the infected tube was incubated at *35–37 ^{0}C*. A color shift from red to yellow, signifying an acidic *PH* alteration, was a sign of a favorable response [38].

Purification of *Myxopyronin B* antibiotic:

This was achieved through the reversed phase chromatography technique. The aeration rate was *0.142 V/ V. min.* The stirring rate was *500 rpm*. *PO2* was at about *90 %* of saturation; but decreased to about *20 %* after *18 hours*]. The fermentation was stopped after *40 hours* via centrifugation at *500 rpm* in a gyrator shaker. The supernatants were collected; and then tested for antimicrobial sensitivity using broth dilution technique to detect *MICs* and agar paper diffusion discs technique. The test antibiotic was extracted from the *2 liters* of culture broth with *2/ 10 volume* ethyl acetate. The ethyl acetate was then removed under the reduced pressure at *40°C*. Afterward, the residue was dissolved in 398 ml of methanol-water [*90:10*] and chromatographed on reversed-phase *HPLC*. Methanol was the mobile phase. The eluent was *70* part *methanol*: *16* part *water*: *and 4* part *acetic acid* with a flow rate of *300 ml/ min*. Detection of the antibiotic components was achieved by exploiting the refractive index. The main peak with a retention time of *5 minutes* contained the biological antibiotic activity which was determined via agar diffusion assay using paper discs and *Staphylococcus aureus* as an indicator organism. On the other hand, the main peak was subjected to neutralization via *NaHCO3*. *Myxopyronin B* was extracted using *10 % V/ V Ethylene chloride*. After the evaporation of the solvent, about *85 %* of the remaining antibiotic substance was pure. It was noticed that the retention time of *Myxopyronin B* was *10 minutes*. The molecular formula of the purified *Myxopyronin B* was detected through a mass spectrometer [Quadrupole mass spectrometer, Advion, USA] [39].

Procedure of *Broth dilution assay* for determination of *MICs* of *Myxopyronin B*: During testing, multiple microtiter plates were filled with a certain broth, according to the needs of the target bacteria. Varying concentrations of the antibiotics and the bacteria to be tested were then added to the plate. The plate was then placed into a non-*CO2* incubator and incubated at thirty-seven degrees Celsius for sixteen to twenty hours. Following the allotted time, the plate was removed and checked for bacterial growth. When the broth became cloudy, bacterial growth occurred. The results of the broth microdilution method were reported in Minimum Inhibitory Concentration [MIC], or the lowest concentration of antibiotics that stopped bacterial expansion [40].

***Agar diffusion assay* with *paper discs* procedure for the determination of *Myxopyronin A* antimicrobial activity:**

The disk diffusion method [*DDM*] was classified as an agar diffusion method [*ADM*] because the test antibiotic extract to be tested diffused from its reservoir through the agar medium seeded with the test microorganism. Generally, the reservoir was a filter paper disk, which was placed on top of an agar surface. When tested extract compounds were microbiologically active, an inhibition zone developed around the filter paper disk after incubation. The diameter of the inhibition zone properly described the antimicrobial potency of the test extract.[41] The test microbes were isolated using either selective or enriched growth media or broth[table 2].

Table [2]. It demonstrates different isolation media for different pathogenic m.os. utilized in the *Broth microdilution* test and agar diffusion assay using paper discs:

Pathogenic m.o	No of strains	Isolation media
Bacillus subtilis	5	Mannitol egg yolk polymixin agar[MEYP]
Bacillus cereus	7	Polymixin egg yolk mannitol bromothymol blue agar[PEMBA]
Staphylococcus aureus	6	Salt mannitol agar[SMA]
Pneumococci	13	Todd Hewitt broth with yeast extract
E. coli	17	Sorbitol- Macconkey agar
Pseudomonas aeruginosa	10	Pseudomonas isolation agar[PSA]
Candida albicans	1	Potato dextrose agar[PDA]
Saccharomyces cerevisiae	5	Sabourad dextrose agar[SDA]
Salmonella typhimurium	4	Bismuth sulfite agar[BSA]
Haemophilus influenza	3	Enriched chocolate agar
Gonococci	4	Thayer martin medium
meningococci	6	Mueller Hinton agar
Serratia Marcescens	4	Caprylate thallous agar medium
Mucor hiemalis	1	Potato dextrose broth
Shigella dysenteriae	8	Hekteon enteric agar
Micrococcus luteus	1	Tryptic soy agar
Proteus mirabilis	1	Blood agar

Estimation of *Myxopyronin B* effect on bacterial *RNA* synthesis:

The concentration of *RNA* isolated with *RNeasy Kits* [purchased from QIAGEN, USA] was determined by measuring the absorbance at *260 nm* in a spectrophotometer. An absorbance of 1 unit at 260 nm corresponds to 40 µg of *RNA* per ml [*A260 = 1 = 40 µg/ ml*] [42].

Estimation of *Myxopyronin B* effect on bacterial protein synthesis:

Absorbance was measured at *205 nm* to calculate the protein concentration by comparison with a standard curve. A [*205*] method could be used to quantify total protein in crude lysates and purified or partially purified protein. The *UV* spectrophotometer was set to read at *205 nm* allowing *15 min* for the instrument to equilibrate. The absorbance reading was set to zero with a solution of the buffer and all components except the protein present. The protein solution was placed in the 1 ml cuvette and the absorbance was determined. The dilution and readings of samples were performed in duplicate. The matched cuvettes for samples and controls were utilized during the test procedure. The extinction coefficient of the protein was known, and the following equation was employed. *Absorbance = Extinction coefficient × concentration of*

protein × *path length* [*1 cm*] to determine the concentration of the protein [43].

Estimation of pharmacodynamic and pharmaco-kinetic effects of *Myxopyronin B* during experimental animal testing in preclinical clinical trials:

In the present study, the pharmacokinetics and the pharmacodynamics of *Myxopyronin A* were evaluated after dosing in 100 male rabbit animal models weighing about *2 kg*. Furthermore, compound concentrations were determined in target compartments, such as lung, kidney, and thigh tissue, using *LC-MS/ MS*. Based on the pharmacokinetic results, the pharmacodynamic profile of *Myxopyronin B* was assessed utilizing the standard neutropenic thigh and lung infection models [44].

Estimation of pharmacodynamic and pharmaco-kinetic effects of *Myxopyronin B* in *randomized human clinical trials phases 1/2*:

This study was conducted on *150* male and female human volunteer subjects with ages ranging from 5-60 years old to show the bioavailability, pharmaco-kinetics, and pharmaco-dynamics of the test antibiotic. The study was designed as a randomized, 500 mg single-dose, *2*-treatment, 2-period crossover trial with a washout period of *1 week*. Blood samples were collected at *0*[*baseline*], *10*, *20*, and *40 minutes* and at *1, 1.5, 2, 3, 4, 6, 9, 12*, and *24 hours* post-dose. Plasma concentrations of the 4 drugs were measured by using a rapid chromatography-tandem mass spectrometry method. Pharmacokinetic parameters were calculated by using non-compartmental methods. Bioequivalence was determined if the *90 % CIs* of the log-transformed test/ reference ratios *AUC* [*0-25*], *AUC* [*0-∞*], and C*max* were within the predetermined range of *80%* to *125%*. Tolerability was assessed by using clinical parameters and subject reports Pharmacodynamic effects were evaluated through the determination of *MICs* via agar diffusion assay and broth dilution technique During randomized human clinical trials phases 1/2 all utilized infectious bacterial cell counts were estimated spectorophotometrically [45].

Estimation of phototoxicity, mutagenicity, and carcinogenicity of *Myxopyronin B*: The phototoxicity was dictated via the *"3T3 neutral red uptake phototoxicity technique"* [46]. On the other hand, mutagenicity and carcinogenicity of the test antibiotic were assessed using *the Ames test* [47].

The determination of *toxicokinetics* and *toxico-dynamics* impacts of *Myxopyronin B*: Up and down method for acute toxicity detection of *Myxopyronin B* was utilized for this purpose [48].

The determination of the maximum bactericidal activity of *Myxopyronin B*: A pure culture of a specified microorganism was grown overnight, then diluted in growth-supporting broth[typically *Mueller Hinton Broth*] to a concentration between *1 x 10^5* and *1 x 10^6 cfu/ ml*. A stock dilution of the antimicrobial test substance was made at approximately *100* times the expected *MIC*. Further *1:1* dilutions were made in test tubes. All dilutions of the test antibiotic were inoculated with equal volumes of the specified microorganism. A positive and negative control tube was included for every test microorganism to demonstrate adequate microbial growth over the course of the incubation period and media sterility, respectively. An aliquot of the positive control was plated and used to establish a baseline concentration of the microorganism used. The tubes were then incubated at the appropriate temperature and duration. Turbidity indicated growth of the microorganism and the *MIC* was the lowest concentration where no growth was visually observed. To determine the *MBC*, the dilution representing the *MIC* and at least two of the more concentrated test product dilutions were plated and enumerated to determine viable *CFU/ ml*. The *MBC* was the lowest concentration that demonstrated a pre-determined reduction [such as 99.9%] in *CFU/ ml* when compared to the *MIC* dilution [49].

Determination of plasma protein binding capacity of *Myxopyronin B*: Using an ultrafiltration technique, the protein binding [*PB*] extent and changeability of the test antibiotic medicates were settled when given simultaneously to *30 patients* inoculated with infectious *pneumococci* inside hospitals in Egypt. Clinical samples used were routinely received by the microbiological laboratory inside the faculty of Pharmacy, Cairo University, Egypt. Plasma proteins were likewise plumbed. A protein-free medium was utilized to ascertain the nonspecific binding. Plasma samples from *30* patients were included, of which plasma proteins were emancipated for *24 patients*.

Determination of liver, kidney, and heart function tests of the test antibiotic: These functional tests were carried out to evaluate the vitality of the liver, kidney, and heart during *the randomized human clinical trials phases 1/2*. On the other hand, Urine, and stool analyses in addition to the estimation of blood complete counts were performed on all experimental subjects given graded doses of *Myxopyronin B*.

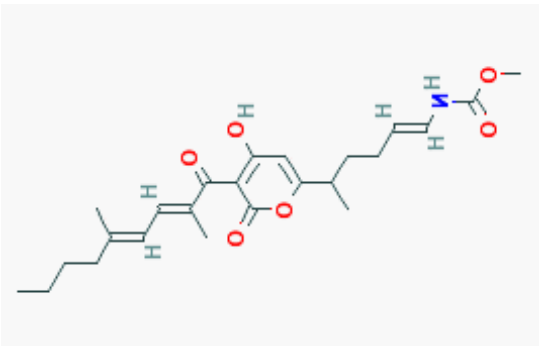

Figure [1]: It demonstrates the structure of *Myxopyronin B* extracted from bacterial isolates *Myxococcus SDU36* collected from different soil environments in Egypt. The molecular formula of the purified test antibiotic was noticed to be $C_{24}H_{33}NO_6$ determined through a mass spectrometer.

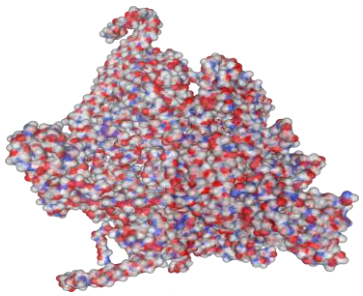

Figure [2]. It represents the docking of *Myxopyronin B* ligand on Bacterial *RNA* polymerase. *Myxopyronin B non-competitively* showed high affinity and inhibitory effect towards the switch region. The molecular mass of *Myxopyronin B* was observed to be nearly *430 Da*. ΔG reached *20 joule/ mole*; while Kd was observed to be nearly *-290 nM*.

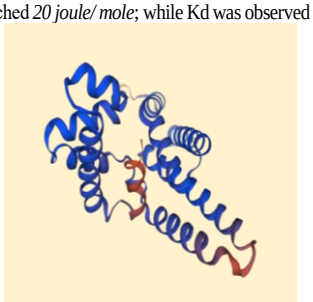

Figure [3]: It demonstrates the 3D structure of bacterial prokaryotic *RNA polymerase* comprising the switch binding site to which *Myxopyronin B Ligand* is strongly bound inhibiting bacterial *RNA polymerase* activity selectively leading to the inhibition of *mRNA* transcription and subsequently the mortality of the microbe. The secondary structure of *the RNA polymerase* enzyme consisted of spiral alpha and beta sheets. Its molecular mass was approximately *198 amino acids*.

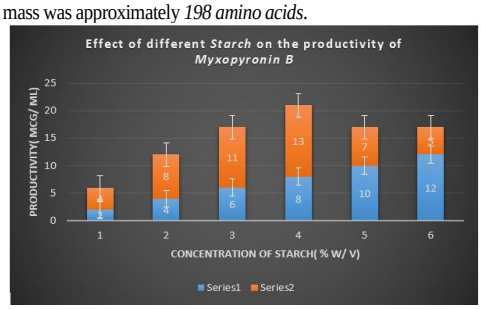

Figure [4]: It shows the impact of various concentrations of *Soluble Starch* on the production of *Myxopyronin B*.

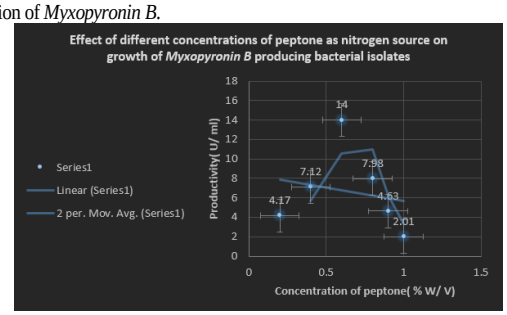

Figure [5]: It shows the effects of different *Peptone* concentrations as nitrogen growth factors on the productivity of *Myxopyronin B*.

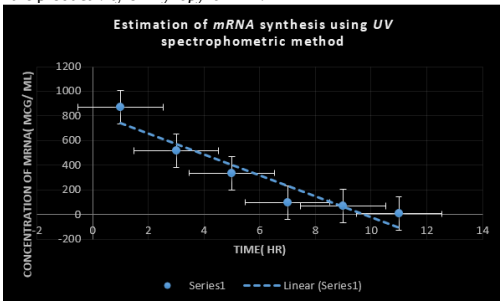

Figure [6]: It refers to the estimation of the effect of *Myxopyronin B* on microbial *mRNA* productivity. *mRNA* synthesis was detected to be diminished proportionately upon employment of exploding doses of *Myxopyronin B* antibiotic.

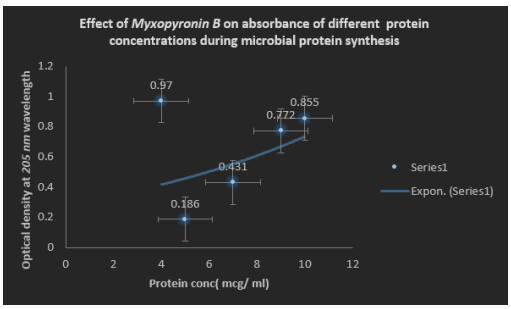

Figure [7]. It demonstrates the influence of *Myxopyronin B* on protein synthesis using *UV* spectrophotometer absorption at *205 nm*. Protein synthesis was noticed to be decreased dramatically upon utilization of increasing doses of *Myxopyronin B* antibiotic.

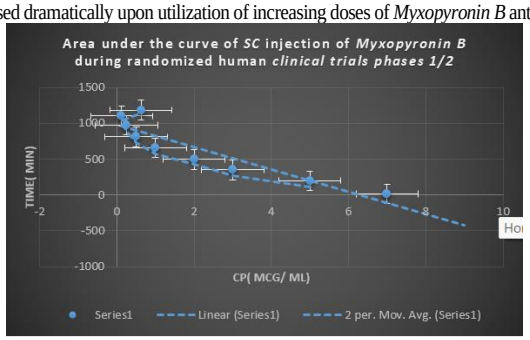

Figure [8]. It shows *the AUC* of *Myxopyronin B* following *SC administration in clinical trial stages 1/2*. Efficacious dose ranged from *7-8 mg/ kg* of body weight. The onset of action was observed following closely *15 minutes*. It followed the first order of elimination kinetics. Bioavailability reached nearly *92%*.

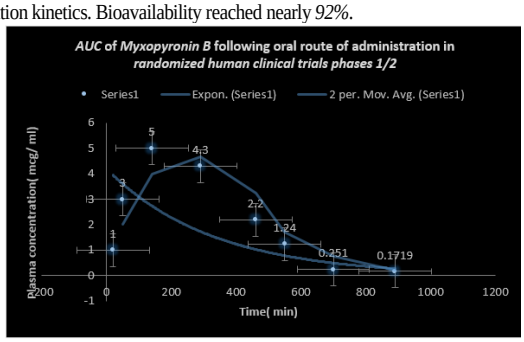

Figure [9]. Area under the curve [*AUC*] following oral administration of *Myxopyronin B* during *clinical trials phases 1/2*. Effective dose ranged from *9-10 mg/ kg* of body weight. The onset of action was observed following nearly *28 minutes*. It followed the first order of elimination kinetics. Bioavailability reached about *90%*.

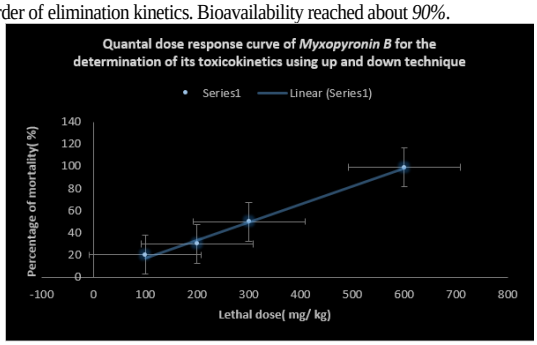

Figure [10]. The quantal dose-response curve for the determination of toxicokinetics of *Myxopyronin B*. *the LD_{50} %* was found to be *300 mg/kg;* while *LD99 %* was nearly *600 mg/ kg.*

Statistical analysis

All cultures were conducted in triplets. Their presentation was by means and standard deviation. One-way analysis of variance [*p value≤ 0.05*] was used as a means for performing statistical analysis and also, statistical analysis was based on excel-spreadsheet-software. The *F statistical analysis test* was utilized during the present study.

Figure [11]. It shows Myxococcus SDU36 bacterial isolates on CYP isolation plates secreting Myxopyronin B antibiotic using a Stereomicroscope.

RESULTS

The primary soil bacterial isolate cultivated on *Casein yeast peptone* plate, *Myxococcus SDU36* produced the culture supernatant from which *Myxopyronin B* was produced. The test antibiotic reduced the growth of a few Gram-ve bacteria, including Escherichia coli, at *MICs* more than *100* mcg/ml, but it did not prevent the development of numerous *Gram+ve* bacteria at *MICs* lower than *100 mcg/ml*. Eukaryotic cells, on the other hand, including those in humans and fungi, were unharmed. The test antibiotic's bactericidal effect was shown by its inhibition of bacterial *DNA-dependent RNA polymerase* [*RNLP*]. In *phase 1/2* of *randomized human clinical trials*, the mean *Cmax* was *9–10 mcg/ml*, and the mean *Tmax* was *1 hour* when the *600 mg* dosage was taken orally. *T1/2* also reached *2.25 hours* after *first-order kinetics* of *elimination*. It took over *eight hours* for it to start working after oral administration. In fewer than *7%* of experimental candidates, rare toxicity in the form of mild diarrhea and *GI* discomfort was found during preclinical and *randomized human clinical trial stages 1/2*. It demonstrated around *90% affinity* to plasma proteins, particularly *Albumin*, which led to a lasting therapeutic effect. It demonstrated an antibiotic's concentration-dependent killing action.

The pace and amount of antimicrobial activity in the concentration-dependent killing pattern increase with drug concentration about the pathogen minimum inhibitory concentration [*MIC*]. After the test antibiotics were refined and purified using *the reverse phase HPLC technology*, *Myxopyronin B* was the predominant component [*Table 4*]. *The 3T3 neutral red uptake phototoxicity test* was used to determine the phototoxicity, and it revealed no phototoxicity. Conversely, *the Ames test* was used to evaluate the mutagenicity and carcinogenicity of the test antibiotic, and the results showed no genotoxicity or carcinogenicity at all.

The quantal dosage response curve for *Myxopyronin B's toxicokinetics* is shown in *Figure 10*. It was discovered that LD_{50}% was *300 mg/kg* and LD_{99}% was over *600 mg/kg*. Using a stereomicroscope, *Figure 11* depicts *Myxococcus SDU36* bacterial isolates on *CYP* isolation plates secreting the antibiotic *Myxopyronin B*.

Tables 9 and 10, show that there was a substantial reduction in protein synthesis and *mRNA* synthesis as the dosage of *Myxopyronin B* was increased. Docking experiments with the *MCULE* and *SWISS DOCK* software showed that the test antibiotic's mode of action was most likely caused by inhibiting *RNA polymerase* by binding to its switch region. The test antibiotic's high ΔG was found to be around *20 J/mol* using the *SWISS model software*. However, utilizing *SWISS-MODEL software*, it was discovered that the test antibiotic's low *Kd* near the switch area was around *-290 nM*. *Table 11* provides a summary of the biochemical profile and morphology of the strong bacterial isolates used in this investigation to produce the test antibiotic. *Myxococcus SDU36* was the most common bacterial isolate found to be secreting the extracellular test antibiotic, according to its morphology and biochemical responses. The study had *150* human volunteers in total, with a mean age of *28.1* [*8.7*] years [*SD*]. The *90%* confidence intervals [*CIs*] for the long-transformed ratios of *Cmax*, *AUC* [*0-25*], and *AUC* [*0-∞*] for the test antibiotic were, respectively, *89.2* to *95.3*, *88.2* to *96.1*, and *90.8* to *93.4*. For *Myxopyronin B*, the mean protein binding [*PB]* was found to be around *90%*. It was shown that albumin exhibited the predominant protein binding for both *Rifampicin* and *Myxopyronin B*. The therapeutic activity was discovered to be attributed to the unbound fraction. The structure of *Myxopyronin B*, which was isolated from bacterial isolates of *Myxococcus SDU36* collected from various soil habitats in Egypt, is depicted in Figure 1. Using a mass spectrometer, the molecular formula of the purified test antibiotic was found to be $C_{24}H_{33}NO_6$. The area under the curve [*AUC*] after oral *Myxopyronin B* dosing throughout *phases 1/2* of *clinical trials* is displayed in *Figure 9*. The range of the effective dosage was *9–10 mg/kg* of body weight. The first signs of activity [onset of action] were noted after about *28 minutes*. It adhered to *the kinetics of first-order elimination*. The location of bacterial isolates that produce *Myxopyronin B* is displayed in *Table 3*. The resolution of biological reactions is shown in Table 11. *Table 10* uses a *UV* spectrophotometer set at *205 nm* to illustrate how *Myxopyronin B* affects the synthesis of microbial proteins. *Table 8* uses the broth microdilution technique to show the minimum bactericidal concentrations [*MBCs*] of *Myxopyronin B* on various bacteria. The estimation of *Myxopyronin B's* impact on microbial *mRNA* productivity is shown in *Figure 6*. An increase in the dosage of the antibiotic *Myxopyronin B* was found to cause a commensurate decrease in *mRNA* production. Following the administration of *Myxopyronin B*, *Table 9* displays the estimation of *mRNA* quantity using a *UV spectrophotometer* at *260 nm*. *Table 7* shows *the broth microdilution technique's* minimum inhibitory concentrations [*MICs*] for several bacteria. *Table 6* illustrates how *the Agar diffusion assay*, which uses *paper discs*, was used to estimate the zones of inhibition and lowest inhibitory doses of *Myxopyronin B*. *Table 5* shows how to use *BLASTn* software to detect isolates that produce *Myxopyronin B* using *16S rRNA*. The range of bacterial isolates that produce *Myxopyronin B* is displayed in *Table 3*. Using a stereomicroscope, *Figure 11* depicts *Myxococcus SDU36* bacterial isolates on *CYP* isolation plates secreting the antibiotic *Myxopyronin B*. The quantal dosage response curve for *Myxopyronin B's toxicokinetics* is shown in *Figure 10*. It was discovered that LD_{50}% was *300 mg/kg* and LD_{99}% was over *600 mg/kg*. The structure of *Myxopyronin B*, which was isolated from bacterial isolates of

Myxococcus SDU36 collected from various soil conditions in Egypt, is depicted in *Figure 1*.

Using a mass spectrometer, the molecular formula of the purified test antibiotic was found to be $C_{24}H_{33}NO_6$. The area under the curve [*AUC*] after oral *Myxopyronin B* dosing during *phases 1/2* of clinical trials is shown in *Figure 9*. The range of the effective dose was *9–10 mg/kg* of body weight. The onset of actions was noted after almost *28* minutes. It adhered to the kinetics of first-order elimination. *The AUC* of *Myxopyronin B* after *SC* injection in *phases 1/2* of clinical trials is displayed in *Figure 8*. The range of effective doses was *7-8 mg/kg* of body weight. The beginning of the action was noted after a close *15* minutes. It adhered to the kinetics of first-order elimination. *Figure 4* illustrates how different soluble starch concentrations affect the synthesis of *Myxopyronin B*. *Figure 7* uses the *UV* spectrophotometer absorption at *205 nm* to illustrate how *Myxopyronin B* affects protein production. A significant reduction in protein synthesis was seen upon administration of escalating dosages of the antibiotic *Myxopyronin B*. *The 3D structure* of bacterial prokaryotic *RNA polymerase* is shown in *Figure 3*. It includes the switch binding site, to which *Myxopyronin B* Ligand binds strongly and inhibits bacterial *RNA polymerase* activity selectively, thereby inhibiting *mRNA* transcription and ultimately causing the microbe to die. *Alpha* and *Beta* spiral sheets make up the *RNA polymerase* enzyme's secondary structure. It had a molecular mass of about *198 amino acids*. The docking of the *Myxopyronin B ligand* on Bacterial *RNA polymerase* is shown in *Figure 2*. High affinity and an inhibitory action were demonstrated by *Myxopyronin B* towards the switch region.

Table [3]. It shows the distribution of Myxopyronin B-producing bacterial isolates:

No of *+ve* bacterial isolates producing *Myxopyronin B*	**No of *-ve* bacterial isolates producing *Myxopyronin B***
42	58

Table [4]. It demonstrates the degree of purity of test antibiotics following the purification via the reversed-phase HPLC technique:

Test antibiotic	**Degree of purity[%]**
Myxopyronin A	*15*
Myxopyronin B	*85*

Table [5]. It demonstrates 16 S rRNA detection of Myxopyronin B-producing isolates using BLASTn software:

Description	Scientific Name	Max Score	Total Score	Query Cover	E value	Per. ident
Myxococcus sp. MH1 DNA, complete genome	*Myxococcus sp. MH1*	525	1051	99%	3.00E-144	94.94
Myxococcus sp. SDU36 chromosome, complete genome	*Myxococcus sp. SDU36*	436	870	99%	1.00E-117	90.15
Myxococcus hansupus strain mixupus chromosome, complete genome	*Myxococcus hansupus*	126	126	65%	3.00E-24	77.23
Cystobacter fuscus strain DSM 52655 chromosome, complete genome	*Cystobacter fuscus*	124	124	54%	1.00E-23	78.92
Cystobacter fuscus strain Cbf 8 chromosome, complete genome	*Cystobacter fuscus*	124	124	54%	1.00E-23	78.92

Table [6]. It shows the estimation of zones of inhibition and minimum inhibitory concentrations of Myxopyronin B via Agar diffusion assay using paper discs:

Test organism[1]	*MIC[µg/ ml]*	Diameter of inhibition zone[*mm*]
Bacillus subtilis	3	11
Staphylococcus aureus	6	17
Streptococcus pneumonae	10	8
Escherichia coli	123	15
Pseudomonas aeruginosa	128	0
Candida albicans	110	0
Sacchromyces cerevisiae	186	0
Salmonella typhimurium	148	14
Bacillus cereus	7	9
Micrococcus luteus	31	15
Serratia Marcescens	187	10
Mucor hiemalis	0	19
Shigella dysentery	192	12
Proteus mirabilis	125	7

The initial density of each organism during the Agar diffusion assay for the determination of minimum inhibitory concentrations and zones of inhibition of growth was nearly 10^5/ ml.

Table [7]. It demonstrates MICs of Myxopyronin B on different microorganisms using broth microdilution technique

Pathogenic m.o	*MIC[µg/ ml]*
Bacillus subtilis	4
Bacillus cereus	2
Staphylococcus aureus	8
Pneumococci	9
E.coli	115
Pseudomonas aeruginosa	139
Candida albicans	0
Saccharomyces cerevisiae	0
Salmonella typhimurium	119
Haemophilus influenza	0
Gonococci	130
meningococci	148
Serratia Marcescens	198
Mucor hiemalis	0
Shigella dysenteriae	166
Micrococcus luteus	0
Proteus mirabilis	157

Table [8]. It demonstrates Minimum bactericidal concentrations [MBCs] of Myxopyronin B on different microorganisms using broth microdilution technique

Pathogenic m.o	***MBC[µg/ ml]***
Bacillus subtilis	30
Bacillus cereus	36
Staphylococcus aureus	45
Pneumococci	31
E.coli	249
Pseudomonas aeruginosa	418
Candida albicans	0
Sacchromyces cerevisiae	0
Salmonella typhimurium	298
Haemophilus influenza	0
Gonococci	401
meningococci	403
Serratia Marcescens	305
Mucor hiemalis	0
Shigella dysenteriae	287
Micrococcus luteus	0
Proteus mirabilis	513

Table [9]. It shows the estimation of mRNA quantity via UV spectrophotometer at 260 nm after addition of Myxopyronin B

***mRNA* concentration[*ng/ ml*]**	***Absorbance[optical density] at 260 nm***
723	0.881
642	0.597
216	0.219
13	0.109

Table [10]. It shows the effect of Myxopyronin B on microbial protein synthesis using a UV spectrophotometer at 205 nm

Bacterial protein concentration[mc*g/ ml*]	**Time[min]**
80.2	60
31.56	180
21.08	300
2.85	450
0.03	720

Table [11]. The resolution of biochemical reactions

Test	Result
Gram stain	-
Cell shape	Elongated bacilli with tapered ends
Spore shape	Ellipsoidal
Spore site	Central
Motility	+ via gliding
Catalase	+
Oxidase	-
Blood haemolysis	-
Indol	-
Methyl red	-
Nitrate reduction test	+
Vogues Proskauer	-
Citrate utilization	-
Starch hydrolysis	+
Casein hydrolysis	+
Growth at 45 ℃	Bacterial isolates did not grow at 45 ℃; but were grown at 10-37 ℃
Tween 80	+
Tolerance salinity	
5% NaCl	-
7% NaCl	-
Saccharide fermentation	
Glucose	-
Fructose	-
Maltose	-
Sucrose	-

DISCUSSION

The in vitro and in vivo antimicrobial activity of *Myxopyronin B*, a novel antibiotic was evaluated in the present study. It demonstrated excellent bactericidal activity against a broad spectrum of *G +ve bacteria* with *MICs* that did not exceed *20 mcg/ ml*. On the other hand, it showed few bactericidal activities against *G -ve bacteria*. With minimal inhibitory concentrations greater than *100 mcg/ ml*. Its mechanism of action was realized during the investigation of *RNA synthesis* to be via the inhibition of prokaryotic *DNA-dependant-RNA polymerase*; whereas no inhibitory impact was observed for Eukaryotic one. Docking studies through *SWISS DOCK* software confirmed this as well. The antibiotic activities *Myxopyronin A* and *B* were isolated from the culture supernatant of *29* bacterial isolates of Myxobacterium *Myxococcus SDU36* detected molecularly using *16 S rRNA* technique [table 3].

The antibiotic activity did not inhibit the growth or kill eukaryotic cells such as human and fungal cells reflecting selectivity towards the inhibition of the growth of prokaryotic bacterial cells. This selectivity effect minimized the adverse effects noticed during the present study. Docking studies via *SWISS DOCK* software revealed that demethylation of either *Myxopyronin A* or *B* enhanced its biological activity. Purification was performed through reversed-phase *HPLC*. *Myxopyronin B* was the main refined antibiotic. Its purity degree reached approximately *85 %*; while the remaining purified antibiotic was detected to be *Myxopyronin A*. The antibacterial activity was assessed via the determination of *MICs* of the test antibiotics using the agar diffusion technique utilizing paper discs *5 mm* in diameter and the broth dilution assay. The initial density of each test microorganism was about 10^5*/ ml* of the culture suspension. The mean *MICs* of test antibiotics against *G +ve bacteria* ranged from *5* to *20 mcg/ ml;* Whereas *MICs* reached above *100 mcg/ ml* against some selected *G -ve bacteria.* Conversely, no effect was detected against the growth of fungi and yeasts. Irschik H *et al.* [39] stated that *myxovalargin A* was a novel peptide antibiotic isolated from the culture supernatant of the *myxobacterium Myxococcus fulvus strain Mx f65*. It was active against *Gram-positive bacteria* [MIC *0.3* approximately *5 micrograms/ ml*], at higher concentrations also against Gram-negative ones [*MIC 6 approximately 100 micrograms/ ml],* and not at all against yeasts and molds. Its mechanism of action involved the inhibition of bacterial protein synthesis [50].

According to Glaus et al. [51], *Ripostatin*, a novel antibiotic, isolated from the culture supernatant of *Myxobacterium*, *Sorangium cellulosum strain Soce377* interfered in the bacterial *RNA* synthesis [51]; whereas *Myxopyronin B* in the present study was found as well to inhibit RNA synthesis. It was structurally related to α-pyrone antibiotics from *myxobacteria*. Its ability to inhibit *RNA polymerase* was through interaction with the switch region of *RNA polymerase*; while *Rifampicin* inhibited the same enzyme through different regions [52].

Myxopyronin B showed no phototoxicity and muta-genicity in rabbit animal models during *the preclinical trials stage*, in the present study. Rare adverse effects including mild

diarrhea and cholestatic jaundice were reported in less than *5 %* of the experimental subjects who received the test antibiotics during *randomized human clinical trials phases 1/2*. The biological half-life of *Myxopyronin A* reached approximately *2.5 hours*. *0.6 % peptone* and 8 *% soluble starch* were detected to be the optimal nitrogen and carbon growth factors for bacterial isolates producing the test antibiotics, respectively [figures 4 and 5]. The high ΔG of the test antibiotic was observed to be approximately *20 J/ mole* as determined via *SWISS-MODEL* software reflecting the high catalytic activity of the test antibiotic towards the switch region. On the other side, low *Kd* of the test antibiotic towards the switch region was found to be approximately *-290 nM* using *SWISS MODEL* software indicating high affinity and binding capacity. Bioavailability studies were performed using *HPLC* during *randomized human clinical trials phases 1/2* revealed that *Myxopyronin B* reached nearly *90% oral bioavailability*, *92% IM bioavailability*, and *100% IV bioavailability*. Metabolic studies using *HPLC* revealed that the test antibiotic showed no in vivo induction of hepatic metabolizing C*ytochrome P450* enzymatic system; while rifampicin induced *CYP3A4* hepatic metabolizing enzyme potently. Up and down procedure intended for the evaluation of the acute toxicity profile of the test antibiotic showed that LD_{50}% was about *200 mg/ kg* body weight; while LD_{99}% reached *300 mg/ kg*. On the other hand, the therapeutic margin of the test antibiotic ranged from *7 mcg/ ml* to *100 mcg/ ml*. *Myxopyronin A*-producing bacterial isolates were gram-negative, spore-forming *obligate aerobes* and *chemoorganotrophic*. They were *elongated rods* with *tapered ends*. No *flagella* were present, but the cells moved via *gliding*. They fermented *Tween 80*, *starch*, and *casein*. On the other hand, they were positive for *catalase* while negative for *oxidase* tests. They reduced *nitrates* and were able to grow at *10-37 °C*. A total of *150* human subjects [mean *SD* age, *27.3* [*9.8*] years were enrolled and completed the study. The *90%* confidence intervals [*CIs*] for the long transformed ratios of *Cmax*, *AUC* [*0-25*], and *AUC* [*0-∞*] for the test antibiotic were, respectively, *89.2* to *95.3*, *88.2* to *96.1*, and *90.8* to *93.4*. The point estimates for *Cmax* in the present study were outside the limit for bio-equivalence for the rifampicin standard drug. The mean PB was observed for *Myxopyronin B* which approximated *90%* while that of *Rifampicin* reached *88%* [53]. It was noticed that plasma protein binding was proportionally increased with increasing the doses of the test antibiotic. The plasma protein binding participated in extending the *Myxopyronin B* duration of action. The major protein binding for *Myxopyronin B* and *Rifampicin* was noticed to be albumin. The unbound fraction was detected to be responsible for the therapeutic activity.

CONCLUSION: Antibiotic resistance is a global challenge that the current study shows promise in solving. According to the findings of the current study, *Myxopyronin B*, which was isolated from the bacterial isolates ΔG was found to be roughly *20 J/mol* using the SWISS *MODEL software*. However, utilizing *SWISS-MODEL software*, it was discovered that the test antibiotic's low *Kd* near the switch area was roughly *-290 nM* that were collected from various soil environments in Egypt, exhibited significant antibiotic activity both in vitro and in vivo against a moderate range of pathogenic bacteria, particularly *G+ve* varieties. Future research is recommended to investigate pharmacological interactions of the synergism type between *Myxopyronin B* and different antibiotic classes.

Financial and non-financial activities and relations of interest: None.

REFERENCES

1. Dalhoff A. Selective toxicity of antibacterial agents-still a valid concept or do we miss chances and ignore risks? Infection. 2021 Feb;49[1]:29-56. DOI: 10.1007/s15010-020-01536-y.

2. Hutchings MI, Truman AW, Wilkinson B. Antibiotics: past, present and future. Curr Opin Microbiol. 2019 Oct; 51:72-80. DOI: 10.1016/j.mib.2019.10.008.

3. Wencewicz TA. Crossroads of Antibiotic Resistance and Biosynthesis. J Mol Biol. 2019 Aug 23; 431[18]:3370-3399. DOI: 10.1016/j.jmb.2019.06.033.

4. Lepe JA, Martínez-Martínez L. Resistance mechanisms in Gram-negative bacteria. Med Intensiva [Engl Ed]. 2022 Jul; 46[7]:392-402. DOI: 10.1016/j.medine.2022.05.004.

5. Vila J, Marco F. Lectura interpretada del antibiograma de bacilos gramnegativos no fermentadores [Interpretive reading of the non-fermenting gram-negative bacilli antibiogram]. Enferm Infecc Microbiol Clin. 2010 Dec;28[10]:726-36. Spanish [English abstract]. DOI: 10.1016/j.eimc.2010.05.001.

6. Mushtaq S, Vickers A, Woodford N, Livermore DM. WCK 4234, a novel diazabicyclooctane potentiating carbapenems against Enterobacteriaceae, Pseudomonas, and Acinetobacter with class A, C, and D β-lactamases. J Antimicrob Chemother. 2017 Jun 1; 72[6]:1688-1695. DOI: 10.1093/jac/dkx035.

7. Irwin SV, Fisher P, Graham E, Malek A, Robidoux A. Sulfites inhibit the growth of four species of beneficial gut bacteria at concentrations regarded as safe for food. PLoS One. 2017 Oct 18; 12[10]:e0186629. DOI: 10.1371/journal.pone.0186629.

8. Jeong S, Lee Y, Yun CH, Park OJ, Han SH. Propionate, together with triple antibiotics, inhibits the growth of Enterococci. J Microbiol. 2019 Nov; 57[11]:1019-1024. DOI: 10.1007/s12275-019-9434-7.

9. Kohanski MA, Dwyer DJ, Hayete B, Lawrence CA, Collins JJ. A common mechanism of cellular death induced by bactericidal antibiotics. Cell. 2007 Sep 7;130(5):797-810. doi: 10.1016/ j.cell.2007.06.049.

10. Brauer M, Herrmann J, Zühlke D, Müller R, Riedel K, Sievers S. Myxopyronin B inhibits growth of a Fidaxomicin-resistant Clostridioides difficile isolate and interferes with toxin synthesis. Gut Pathog. 2022 Jan 6;14(1):4. doi: 10.1186/ s13099-021-00475-9.

11. Doundoulakis T, Xiang AX, Lira R, Agrios KA, Webber SE, Sisson W, et al. Myxopyronin B analogs as inhibitors of RNA polymerase, synthesis and biological evaluation. Bioorg Med Chem Lett. 2004 Nov 15;14(22):5667-72. doi: 10.1016/j.bmcl.2004.08.045.

12. Lira R, Xiang AX, Doundoulakis T, Biller WT, Agrios KA, Simonsen KB, et al.. Syntheses of novel myxopyronin B analogs as potential inhibitors of bacterial RNA polymerase. Bioorg Med Chem Lett. 2007 Dec 15;17(24):6797-800. doi: 10.1016/j.bmcl.2007.10.017.

13. Moy TI, Daniel A, Hardy C, Jackson A, Rehrauer O, Hwang YS, et al. Evaluating the activity of the RNA polymerase inhibitor myxopyronin B against Staphylococcus aureus. FEMS Microbiol Lett. 2011 Jun;319(2):176-9. doi: 10.1111/j.1574-6968.2011.02282.x.

14. Srivastava A, Talaue M, Liu S, Degen D, Ebright RY, Sineva E, et al. New target for inhibition of bacterial RNA polymerase: 'switch region'. Curr Opin Microbiol. 2011 Oct;14(5):532-43. doi: 10.1016/j.mib.2011.07.030.

15. Mosaei H, Harbottle J. Mechanisms of antibiotics inhibiting bacterial RNA polymerase. Biochem Soc Trans. 2019 Feb 28;47(1):339-350. doi: 10.1042/BST20180499.

16. Sucipto H, Sahner JH, Prusov E, Wenzel SC, Hartmann RW, Koehnke J, Müller R. *In vitro* reconstitution of α-pyrone ring formation in myxopyronin biosynthesis. Chem Sci. 2015 Aug 1;6(8):5076-5085. doi: 10.1039/c5sc01013f.

17. O'Toole GA. Classic Spotlight: How the Gram Stain Works. J Bacteriol. 2016 Nov 4;198(23):3128. doi: 10.1128/JB.00726-16.

18. Luhur J, Chan H, Kachappilly B, Mohamed A, Morlot C, Awad M, et al. A dynamic, ring-forming MucB / RseB-like protein influences spore shape in Bacillus subtilis. PLoS Genet. 2020; 16[12]:e1009246. doi: 10.1371/journal.pgen.1009246.

19. Qin Y, Faheem A, Hu Y. A spore-based portable kit for on-site detection of fluoride ions. J Hazard Mater. 2021 Oct 5;419:126467. doi: 10.1016/j.jhazmat.2021.126467.

20. Cabeen MT, Jacobs-Wagner C. Bacterial cell shape. Nat Rev Microbiol. 2005;3(8):601-10. doi: 10.1038/nrmicro1205.

21. Wang Q, Xiao L, He Q, Liu S, Zhang J, Li Y, et al. Comparison of hemolytic activity of tentacle-only extract from jellyfish Cyanea capillata in diluted whole blood and erythrocyte suspension: diluted whole blood is a valid test system for hemolysis study. Exp Toxicol Pathol. 2012 Nov;64[7-8]:831-5. doi: 10.1016/j.etp.2011.03.003.

22. Dubay MM, Acres J, Riekeles M, Nadeau JL. Recent advances in experimental design and data analysis to characterize prokaryotic motility. J Microbiol Methods. 2023 Jan;204:106658. doi: 10.1016/j.mimet.2022.106658.

23. Wang C, Zhang Y, Luo H, Zhang H, Li W, Zhang WX, Yang J. Iron-Based Nanocatalysts for Electrochemical Nitrate Reduction. Small Methods. 2022 Oct; 6[10]:e2200790. doi: 10.1002/smtd.202200790.

24. Hu CY, Cheng HY, Yao XM, Li LZ, Liu HW, Guo WQ, Yan LS, Fu JL. Biodegradation and decolorization of methyl red by *Aspergillus versicolor* LH1. Prep Biochem Biotechnol. 2021;51[7]:642-649. doi: 10.1080/10826068.2020.1848868.

25. Xu D, Wu L, Yao H, Zhao L. Catalase-like nanozymes: Classification, Catalytic Mechanisms, and Their Applications. Small. 2022 Sep;18[37]:e2203400. doi: 10.1002/smll.202203400.

26. Pawlik A, Stefanek S, Janusz G. Properties, Physiological Functions and Involvement of Basidiomycetous Alcohol Oxidase in Wood Degradation. Int J Mol Sci. 2022 Nov 9;23[22]:13808. doi: 10.3390/ijms232213808.

27. Cordaro JT, Sellers W. Blood coagulation test for citrate utilization. Appl Microbiol. 1968 Jan; 16[1]:168-9. doi: 10.1128/am.16.1.168-169.1968.

28. Krajang M, Malairuang K, Sukna J, Rattanapradit K, Chamsart S. Single-step ethanol production from raw cassava starch using a combination of raw starch hydrolysis and fermentation, scale-up from 5-L laboratory and 200-L pilot plant to 3000-L industrial fermenters. Biotechnol Biofuels. 2021 Mar 16; 14[1]:68. doi: 10.1186/s13068-021-01903-3.

29. Kerwin BA. Polysorbates 20 and 80 used in the formulation of protein biotherapeutics: structure and degradation pathways. J Pharm Sci. 2008 Aug;97[8]:2924-35. doi: 10.1002/jps.21190.

30. Trueba FJ, Neijssel OM, Woldringh CL. Generality of the growth kinetics of the average individual cell in different bacterial populations. J Bacteriol. 1982 Jun;150[3]:1048-55. doi: 10.1128/jb.150.3.1048-1055.1982.

31. McCrea KW, Xie J, LaCross N, Patel M, Mukundan D, Murphy TF, Marrs CF, Gilsdorf JR. Relationships of non-typeable Haemophilus influenzae strains to hemolytic and nonhemolytic Haemophilus haemolyticus strains. J Clin Microbiol. 2008 Feb; 46[2]:406-16. doi: 10.1128/JCM.01832-07.

32. Jogawat A, Vadassery J, Verma N, Oelmüller R, Dua M, Nevo E, Johri AK. PiHOG1, a stress regulator MAP kinase from the root endophyte fungus Piriformospora indica, confers salinity stress tolerance in rice plants. Sci Rep. 2016 Nov 16;6:36765. doi: 10.1038/srep36765.

33. Barry AL, Feeney KL. Two quick methods for the Voges-Proskauer test. Appl Microbiol. 1967 Sep;15[5]:1138-41. doi: 10.1128/am.15.5.1138-1141.1967.

34. Wang J, Su Y, Jia F, Jin H. Characterization of casein hydrolysates derived from enzymatic hydrolysis. Chem Cent J. 2013 Apr 4;7[1]:62. doi: 10.1186/1752-153X-7-62.

35. de Bie TH, Witkamp RF, Balvers MG, Jongsma MA. Effects of γ-aminobutyric acid supplementation on glucose control in

adults with prediabetes: A double-blind, randomized, placebo-controlled trial. Am J Clin Nutr. 2023 Sep; 118[3]:708-719. doi: 10.1016/j.ajcnut.2023.07.017.

36. Endoh R, Horiyama M, Ohkuma M. D-Fructose Assimilation and Fermentation by Yeasts Belonging to Saccharomycetes: Rediscovery of Universal Phenotypes and Elucidation of Fructophilic Behaviors in *Ambrosiozyma platypodis* and *Cyberlindnera americana*. Microorganisms. 2021 Apr 5;9[4]:758. doi: 10.3390/microorganisms9040758.

37. Lu Z, Guo W, Liu C. Isolation, identification and characterization of novel Bacillus subtilis. J Vet Med Sci. 2018 Mar 24;80[3]:427-433. doi: 10.1292/jvms.16-0572.

38. Zhao Y, Meng K, Fu J, Xu S, Cai G, Meng G, Nielsen J, Liu Z, Zhang Y. Protein engineering of invertase for enhancing yeast dough fermentation under high-sucrose conditions. Folia Microbiol [Praha]. 2023 Apr;68[2]:207-217. doi: 10.1007/s12223-022-01006-y.

39. Irschik H, Gerth K, Höfle G, Kohl W. The myxopyronins, new inhibitors of bacterial RNA synthesis from Myxococcus fulvus [Myxobacterales]. J Antibiot [Tokyo]. 1983; 36[12]: 1651-8. doi: 10.7164/antibiotics.36.1651.

40. Wiegand I, Hilpert K, Hancock RE. Agar and broth dilution methods to determine the minimal inhibitory concentration [MIC] of antimicrobial substances. Nat Protoc. 2008; 3[2]:163-75. doi: 10.1038/nprot.2007.521.

41. Balouiri M, Sadiki M, Ibnsouda SK. Methods for *in vitro* evaluating antimicrobial activity: A review. J Pharm Anal. 2016 Apr;6[2]:71-79. doi: 10.1016/j.jpha.2015.11.005.

42. Dell'Anno A, Fabiano M, Duineveld GCA, Kok A, Danovaro R. Nucleic acid [DNA, RNA] quantification and RNA/DNA ratio determination in marine sediments: comparison of spectrophotometric, fluorometric, and high-performance liquid chromatography methods and estimation of detrital DNA. Appl Environ Microbiol. 1998 Sep; 64[9]:3238-45. doi: 10.1128/AEM.64.9.3238-3245.1998.

43. Simonian MH. Spectrophotometric determination of protein concentration. Curr Protoc Cell Biol. 2002 Aug;Appendix 3:Appendix 3B. doi: 10.1002/0471143030.cba03bs15.

44. Rox K, Becker T, Schiefer A, Grosse M, Ehrens A, Jansen R, et al. Pharmacokinetics and Pharmacodynamics [PK/PD] of Corallopyronin A against Methicillin-Resistant *Staphylococcus aureus*. Pharmaceutics. 2022 Dec 30;15[1]:131. doi: 10.3390/pharmaceutics15010131.

45. Xu J, Jin H, Zhu H, Zheng M, Wang B, Liu C, et al. Oral bioavailability of rifampicin, isoniazid, ethambutol, and pyrazinamide in a 4-drug fixed-dose combination compared with the separate formulations in healthy Chinese male volunteers. Clin Ther. 2013 Feb;35[2]:161-8. doi: 10.1016/j.clinthera.2013.01.003.

46. Utku Türk EG, Jannuzzi AT, Alpertunga B. Determination of the Phototoxicity Potential of Commercially Available Tattoo Inks Using the 3T3-neutral Red Uptake Phototoxicity Test. Turk J Pharm Sci. 2022 Feb 28;19[1]:70-75. doi: 10.4274/tjps.galenos.2021.86344.

47. Thomas DN, Wills JW, Tracey H, Baldwin SJ, Burman M, Williams AN, et al. Ames Test study designs for nitrosamine mutagenicity testing: qualitative and quantitative analysis of key assay parameters. Mutagenesis. 2023 Dec 19:gead033. doi: 10.1093/mutage/gead033.

48. Zhang YY, Huang YF, Liang J, Zhou H. Improved up-and-down procedure for acute toxicity measurement with reliable LD_{50} verified by typical toxic alkaloids and modified Karber method. BMC Pharmacol Toxicol. 2022 Jan 4;23(1):3. doi: 10.1186/s40360-021-00541-7.

49. Heuser E, Becker K, Idelevich EA. Bactericidal Activity of Sodium Bituminosulfonate against *Staphylococcus aureus*. Antibiotics [Basel]. 2022 Jul 5;11[7]:896. doi: 10.3390/antibiotics11070896.

50. Irschik H, Gerth K, Kemmer T, Steinmetz H, Reichenbach H. The myxovalargins are new peptide antibiotics from Myxococcus fulvus [Myxobacterales]. I. Cultivation, isolation, and some chemical and biological properties. J Antibiot [Tokyo]. 1983 Jan; 36[1]:6-12. doi: 10.7164/antibiotics.36.6.

51. Glaus F, Dedić D, Tare P, Nagaraja V, Rodrigues L, Aínsa JA, et al. Total Synthesis of Ripostatin B and Structure-Activity Relationship Studies on Ripostatin Analogs. J Org Chem. 2018 Jul 6;83[13]:7150-7172. doi: 10.1021/acs.joc.8b00193.

52. Dennison TJ, Smith JC, Badhan RKS, Mohammed AR. Formulation and Bioequivalence Testing of Fixed-Dose Combination Orally Disintegrating Tablets for the Treatment of Tuberculosis in the Paediatric Population. J Pharm Sci. 2020; 109[10]:3105-3113. doi: 10.1016/j.xphs.2020.07.016.

53. Alghamdi WA, Al-Shaer MH, Peloquin CA. Protein Binding of First-Line Antituberculosis Drugs. Antimicrob Agents Chemother. 2018 Jun 26;62[7]:e00641-18. doi: 10.1128/AAC.00641-18.

IJMA

International Journal of Medical Arts

VOLUME 6, ISSUE 8, AUGUST 2024

P- ISSN: 2636-4174
E- ISSN: 2682-3780